Active and Inactive Genes Localize Preferentially in the Periphery of Chromosome Territories

Anette Kurz,* Stefan Lampel,* Jeremy E. Nickolenko,* Joachim Bradl,‡§ Axel Benner,‖ Rebekka M. Zirbel,* Thomas Cremer,‡ and Peter Lichter*

*Abteilung Organisation komplexer Genome, Deutsches Krebsforschungszentrum, D-69120 Heidelberg, Germany; ‡Institut für Humangenetik und Anthropologie, Universität Heidelberg, Heidelberg, Germany; §Institut für Angewandte Physik, Universität Heidelberg, Heidelberg, Germany; and ‖Abteilung Biostatistik, Deutsches Krebsforschungszentrum, Heidelberg, Germany

Abstract. The intranuclear position of a set of genes was analyzed with respect to the territories occupied by the whole chromosomes in which these genes are localized. Genes and their respective chromosome territories were simultaneously visualized in three-dimensionally preserved nuclei applying dual color fluorescence in situ hybridization. Three coding (*DMD*, *MYH7*, and *HBB*) and two noncoding sequences (D1Z2 and an anonymous sequence) were analyzed in four different cell types, including cells where *DMD* and *MYH7* are actively transcribed. Spatial analysis by confocal laser scanning microscopy revealed that the genes are preferentially located in the periphery of chromosome territories. This positioning was independent from the activity of the genes. In contrast, the non-expressed anonymous fragment was found randomly distributed or localized preferentially in the interior of the corresponding chromosome territory. Furthermore, the distribution of the analyzed genes within the territorial peripheries was found to be highly characteristic for each gene, and, again, independent from its expression. The impact of these findings with regard to the three-dimensional arrangement of the linear DNA string within chromosome territories, as well as with respect to a putative nuclear subcompartment confining gene expression, are discussed.

D
ESPITE intensive efforts to decode the linear structure of complex genomes, up to the present day little is known about the three-dimensional genome organization within the cell nuclei of higher organisms. A territorial organization of interphase chromosomes has already been postulated by early cytologists such as Carl Rabl and Theodor Boveri (for review see Cremer, 1985), but this concept was mainly ignored in the 1960's and 70's (see e.g., Comings, 1980). The territorial organization was first shown indirectly by experiments, in which damaged regions of microirradiated cell nuclei, visualized in the subsequently prepared metaphase chromosomes, were found to be locally clustered (Zorn et al., 1979; Cremer et al., 1982). The chromosome territories were later visualized directly by means of in situ hybridization in interspecies somatic hybrid cells (Manuelidis, 1985; Schardin et al., 1985). Application of chromosome painting protocols subsequently proved that territorial organization of chromosomes occurs also in nonhybrid cells of mammalian (Cremer et al., 1988; Lichter et al., 1988*a,b*;

Pinkel et al., 1988) and plant (Schwarzacher et al., 1989; Leitch et al., 1990) origin. However, the spatial organization of the linear DNA molecule within a chromosome territory remains unclear. Based on the analysis of nuclear distances between DNA segments from the same chromosome, it has been suggested that the spatial position of chromatin segments within a chromosome territory follows a random distribution (van den Engh et al., 1992; Yokota et al., 1995; Sachs et al., 1995).

The view of a functionally important role for intranuclear positioning of chromatin at various levels of organization in transcription and differentiation has been debated extensively (see for example Comings, 1968; Vogel and Schroeder, 1974; Heslop-Harrison and Bennett, 1984; Manuelidis, 1984; Blobel, 1985; Gasser and Laemmli, 1987; Belmont et al., 1989; Hilliker and Appels, 1989; Arndt-Jovin et al., 1990; Haaf and Schmid, 1991). A number of observations have been made regarding the dynamics of the spatial arrangement of chromatin regions dependent on cell cycle stages (Ferguson and Ward, 1992), terminal cell differentiation (Graham, 1954; Schmid and Krone, 1976; Manuelidis, 1984), and pathological influences (Barr and Bertram, 1951; Bertram, 1966; Borden and Manuelidis, 1988; Brasch, 1990). These strongly support the view of a specific intranuclear chromatin positioning.

Please address all correspondence to P. Lichter, Abteilung Organisation komplexer Genome, DKFZ, Im Neuenheimer Feld 280, 69120 Heidelberg, Germany. Tel.: 49 6221 424 609. Fax: 49 6221 424 639. E-mail: p.lichter @dkfz-heidelberg.de

In analogy to the fact that r-DNA is localized and transcribed in the nucleolus, where the biogenesis of the ribosome subunits takes place, it has been postulated that other functional nuclear compartments exist (see for example Blobel, 1985; Nyman et al., 1986; Hochstrasser and Sedat, 1987; Manuelidis, 1990; Spector, 1990; Carter et al., 1991). Although the localization of DNAse hypersensitive sites in the nuclear periphery led to the conclusion that active genes transcribed by RNA-polymerase II are preferentially localized in these regions (Hutchison and Weintraub, 1985), this observation could not be confirmed by others (Manuelidis and Borden, 1988). Furthermore, the direct visualization of nuclear components which are involved in processes of gene expression, such as formation of transcription complexes, RNA-transcription, and posttranscriptional RNA processing, have, in general, not revealed a predominant localization in the nuclear periphery (e.g., Spector, 1990; Lawrence et al., 1988; Carmo-Fonseca et al., 1991; Jackson et al., 1993; Wansink et al., 1993). Such a localization was reported for intron sequences of one RNA species (Berman et al., 1990), but this analysis is concerned only with a single gene and the spatial association of these intron RNA sequences with the respective gene is not known. Thus, it remains to be determined whether there is a specific intranuclear positioning of genes, which are transcribed by RNA-polymerase II.

In concordance with the concept of function-specific nuclear subcompartments, RNA transcripts have been found highly accumulated in the nucleus (Berman et al., 1990; Lawrence et al., 1989; Huang and Spector, 1991; Raap et al., 1991; Jiménez-Garcia and Spector, 1993; Zirbel et al., 1993). After visualization by in situ hybridization, these RNA concentrations were seen as punctate spots or track-like objects. Simultaneous visualization of such RNA concentrations and the chromosome territories harboring the respective genes indicated that the RNA signal is generally localized at the chromosome territory surface (Zirbel et al., 1993). Similarly, investigation of the three-dimensional arrangement of chromosome territories and splicing snRNPs by combination of in situ hybridization and immunodetection protocols revealed that the accumulations of the splicing snRNPs are basically excluded from the interior of chromosome territories (Zirbel et al., 1993).

Here we report an analysis of the spatial localization of coding and noncoding sequences within three-dimensionally conserved chromosome territories and the comparison of gene topology when these genes are actively transcribed or inactive. Implications of the results regarding more general models of the nuclear organization of complex genomes are discussed.

Materials and Methods

Cells

HeLa cells and human primary fibroblasts were cultured in DMEM medium supplemented with 10% FCS and primary human myoblasts in Ham's F-10 medium supplemented with 15% FCS and 0.5% chicken embryo extract in collagen-coated flasks. Fusion of myoblasts, grown to confluency to syncythial myotubes was induced by replacing medium with DMEM supplemented with 4.5 g/l glucose, 2% horse serum, and 0.1 mM insulin. 7–10 d after growth in the fusion medium, 63–90% of myoblasts had fused and become myotubes containing 3–50 nuclei.

Homogeneity of the myoblast cell population was tested by indirect immunofluorescence against the muscle cell-specific intermediate filament protein desmin: Cells were fixed in ice cold methanol:aceton (1:1) for 20 min followed by blocking with FCS. After incubation with mouse anti-desmin antibody (5 μg/ml in PBS; Boehringer Mannheim Corp., Indianapolis, IN), cells were incubated with FITC-conjugated anti–mouse antibody (12 μg/ml in PBS; Boehringer Mannheim) for 1 h at 37°C. After counterstaining the cell nuclei with propidium iodide (200 ng/ml in PBS), desmin could be detected in the cytoplasm of 97.5% of the tested cell population.

Probes

Painting of the total human chromosomes 1, 11, and X was achieved using DNA libraries pBS 1, pBS 11 (Collins et al., 1991), and LA0XNL01 (Amer. Type Culture Collection, Rockville, MD), respectively.

The pBS libraries were generously provided by J. Gray (UCSF, San Francisco, CA). Chromosome 14 was delineated after IRS-PCR from the mouse–human hybrid cell line GM 10479 (Human Genetic Cell Repository, Camden, NJ) as described (Lichter et al., 1990a). The only human material in this cell line was chromosome 14 as shown by dual color in situ hybridization with pBS 14 and total human DNA as probes (not shown).

The genes dystrophin (DMD),[1] β-myosin HC (MYH7), and β-globin (HBB) were detected by genomic probes: DMD by a pool of five genomic cosmid clones containing sequences of the region from exon 42 to exon 51 (Tocharoentanaphol et al., 1994), MYH7 by a pool of four plasmids subcloned from the clone λgMHC-1 (Lichter et al., 1986), and HBB by cosmid clone K 40 (Collins and Weissman, 1984) which contains the human β-globin cluster HBBC. Probe D1Z2 recognizes a repetitive sequence cluster in chromosome band 1p36 (Buroker et al., 1987). Cosmid probe 4-4B contains an anonymous genomic DNA fragment from band 11q14 (Lichter et al., 1990b) for which no coding information could be identified (see below). Probe DNAs for painting of total chromosomes were labeled with digoxigenin and probe DNAs for genes and noncoding DNA sequences with biotin by nick-translation as previously described (Lichter et al., 1990b).

All probes detected >95% of their target sequences, i.e., more than 95% of the cell nuclei of diploid cells, showed both homologous loci simultaneously with both chromosome territories.

Analysis of Gene Expression

The expression of the genes DMD, MYH7, HBB, and β-actin (ACTB) was analyzed by RT-PCR. RNA was extracted from HeLa cells, fibroblasts, myoblasts, and 10-d-old myotubes according to standard protocols (Sambrook et al., 1989). 1 μg total RNA from each tested cell population was transcribed into cDNA by reverse transcriptase (AMV, 12 U; Boehringer Mannheim) for 1 h at 42°C using random hexamers (100 pM) as primers and dNTP's (1 mM each). After adding the respective upstream and downstream PCR primers (40 pM each) and Taq Pol (2.5 U; Cetus Corp., Berkeley, CA), the amplification was initiated by denaturation for 3 min at 95°C. Conditions for 30 cycles of amplification for ACTB and HBB sequences were as follows (in brackets conditions for DMD and MYH7): Synthesis at 72°C: 1 min 40 s (30 s); denaturation at 95°C: 2 min (1 min); primer annealing at 55°C: 2 min (30 s). The PCR products were purified (PCR purification kit, Diagen, Hilden, Germany) and analyzed in an agarose-gel (3%, NuSieve 3:1). In each case PCR primers were chosen to be from different exons with one or two introns in between. PCR products originating from spliced RNA template were visible as fragments with a length calculated from sequence data (for primers and references see Table I).

To test if cosmid 4-4B contains expressed sequences, a Northern blot analysis was performed as described (Sambrook et al., 1989) using total RNA isolated from cultures of HeLa cells, primary human fibroblasts, primary human myoblasts, and myotubes 8 d after induction. Cosmid-DNA and β-actin control DNA were labeled radioactively. 50 ng of cosmid DNA was combined with 75 μg Cot-1 DNA, denatured and preannealed for 4 h at 65°C before hybridization. Posthybridization washes were performed to a stringency of 2 × SSPE, 0.1% SDS at room temperature. After exposure to an X-ray film, the filter was rehybridized with ACTB control DNA including posthybridization washes to a stringency of 0.1 × SSPE, 0.1% SDS at 65°C.

---

1. Abbreviations used in this paper: ACTB, human β-actin gene; DMD, human dystrophin gene; FISH, fluorescence in situ hybridization; HBB, human β-globin gene.

Table I. Characteristics of the Analyzed Genetic Loci

Loci	Localization	Probes	RT-PCR Primer
DMD	Xp21.3-p21.2 (Lindenbaum et al., 1979)	Pool of five cosmid clones: TM 4, TM 5, TM 7, TM 13, TM 14 (Tocharoentanaphol et al., 1994)	5'-AGTGCTCCCATAAGCCCAGA-3' (exon 47) 5'-AACGTCAAATGGTCCTTCTT-3' (exon 48) (Ehrenpreis et al., 1991)
MYH7	14q11.2-q13 (Matsuoka et al., 1989)	Pool of four genomic subclones (pSC-C, pSC-D, pSC-E, pSC-F) from the λgMHC-1 clone (Lichter et al., 1986)	5'-TTGGTCATCAGCTTGTTCAG-3' (exon 18) 5'-ACTATGCTGGGGCTGATGCG-3' (exon 16) (Junkes-Biehl, 1992)
HBB	11p15.5 (Morton et al., 1984)	Cosmid clone K 40 containing the gene cluster HBBC (Collins and Weissman, 1984)	5'-GGTGAACGTGGATGAAGTTG-3' (exon 1) (Complementary to PC 04, Saiki et al., 1985) 5'-ACTCAGTGTGGCAAAGGTGC-3' (exon 2) (Spiegelberg et al., 1989)
D1Z2	1p36.3 (Buroker et al., 1987)	Plasmid clone D1Z2 (Buroker et al., 1987)	
"4-4B" designation of probe	11p14 (Lichter et al., 1990b)	Cosmid clone 4-4B (Lichter et al., 1990b)	
ACTB		Plasmid clone pHF β A-1 (Gunning et al., 1983)	5'-GTGGGGCGCCCCAGGCACCA-3' (exon 1) 5'-CTCTTGCTCTGGGCCTCGTC-3' (exon 2) (Akoury et al., 1993)

Cellular Preparations

For in situ hybridization, cells were grown on glass slides, which were collagen-coated for myoblast and myotube cultures. Preparations preserving the three-dimensional structure of the cells were performed as follows: Cells were washed in PBS (37°C) at room temperature and fixed with 4% buffered paraformaldehyde (10 min). Permeabilization to facilitate probe penetration was achieved by incubation with 0.1 M HCl (10 min), then with 0.5% Triton X-100 and 0.5% saponin in PBS (10 min), and finally, after equilibration in 20% glycerol/ PBS (20 min) by freezing them once in liquid nitrogen. After thawing, cells were stored in PBS. Cells were not allowed to dry at any time. This fixation and permeabilization procedure was the best of a series of tested protocols. It gave optimal results combining the preservation of the cellular 3D-structure with the fluorescence in situ hybridization (FISH) procedure (see below and Results).

Fluorescence In Situ Hybridization

Dual color chromosomal in situ suppression hybridization was performed as described (Lichter et al., 1990b). Denaturation of fixed and permeabilized cells was performed in 70% formamide, 2 × SSC, 50 mM sodium phosphate, pH 7.0, at 73°C for 3 min followed by incubation in 50% formamide, 2 × SSC, 50 mM sodium phosphate, pH 7.0, for 1 min at 73°C before applying the hybridization cocktail. Preannealing of denatured probe was allowed for 10 min, except for probe D1Z2 that was denatured separately and chilled on ice. Hybridization was allowed to proceed overnight at 37°C. After posthybridization washes, chromosomal territories were visualized via anti–digoxigenin-rhodamine and the genetic loci via avidin-FITC.

Microscopic Evaluation

Fluorescently labeled specimen were analyzed by confocal laser scanning microscopy (LSM), using an LSM 10 (Zeiss). FITC and rhodamine signals were detected after excitation with the 488-nm line of an argon ion laser and the 543-nm line of a helium neon laser, respectively. The parameters for acquisition of digitized images presenting optical sections were chosen such that the fluorescent signals seen on the screen corresponded closely in size and shape to the pictures seen by conventional fluorescence microscopy. After serial sectioning throughout the nucleus, the plane in which the spotlike FITC signal was focused was identified. Confocal images of FITC and rhodamine fluorescence were taken sequentially in the same focal plane and overlayed electronically (performed for analysis of DMD, MYH7, and HBB). After upgrading the LSM and the installment of a second photomultiplier, the FITC and rhodamine images were simultaneously acquired (performed for the analysis of D1Z2 and 4-4B). Throughout the whole study, alignment of both laser lines were regularly tested to avoid the possible influence of voxel shifts as much as possible. This test was performed by imaging the signals derived from the DMD probe which was simultaneously detected via FITC and rhodamine: after overlaying both images, the signals did not accurately match if the two laser lines were re-aligned.

Test for the Preservation of Nuclear Architecture

The integrity of cellular and chromatin structure after fixation with 4% paraformaldehyde, HCl permeabilization, denaturation, and FISH was tested: After a more modest fixation with 2% paraformaldehyde, kinetochores were stained by indirect immunofluorescence using CREST serum and FITC-conjugated anti–human antibodies. Optical sections of nuclei containing FITC signals derived from the kinetochores were acquired by a confocal LSM and stored. Subsequently, the same cells were fixed with 4% paraformaldehyde, treated with saponin/Triton X-100 and HCL as well as liquid nitrogen to permeabilize cells (see above), and hybridized with a digoxigenin-labeled DNA probe targeting all centromeres (Dunham et al., 1992). Images of the hybridization signals obtained via anti–digoxigenin-conjugated rhodamine were acquired from the same focal plane in the same nuclei as before. Analysis of the preservation of the spatial arrangement of centromeres in the nucleus was performed by overlaying FITC and rhodamine images and assessing the colocalization of individual signals in both sections.

Digital Image Analysis

A subset of images of chromosome territories was interactively segmented by two independent investigators in order to (a) compare the size and shape of segmented chromosome territories (b) to test in a blind fashion whether the signals of the short DNA sequences are located inside the chromosomal domain or at their periphery; and (c) to calculate the interior and exterior areas of chromosome territories. First, the chromosome territory images (rhodamine) were interactively segmented without knowledge of the position of the signal from the corresponding genetic locus. Then, the image with the segmented chromosome territory was electronically overlayed with the image of the FITC signals derived from the same focal plane (see above). Assessment of the localization of an FITC signal in an exterior or interior area of a chromosome territory was achieved as follows (illustrated in Fig. 4): the signal is at the surface of the territory if the center of the signal is inside or outside of the territory border by not more than the diameter (0.5–0.8 μm) of the signal (exterior area); and the signal is within a territory, if it is inside the region defined as the surface (interior area). After these criteria, the computer program decided whether the signal was located inside or in the periphery, or even outside of the territory. Likewise the size of the exterior and interior areas were calculated (see Table II).

The exterior area was further subdivided into two regions, one facing and one not-facing the nuclear boundary (see Fig. 6 A). These two subregions were defined in the following way: The point within the exterior area, which is closest to the nuclear boundary, was determined; the tangent through this closest point and its parallel on the inner nuclear side with the distance given by the diameter of the locus signal (0.5–0.8 μm)

Table II. Concordance of Interactive Segmentation of Chromosome Territories by Two Investigators A and B

Cell type and chromosome territory	Myoblasts chromosome 11	Fibroblasts chromosome 11	HeLa cells X chromosome
	$n = 26$	$n = 61$	$n = 25$
	A: E = 42%	A: E = 45.5%	A: E = 54%
Exterior (E) and	I = 58%	I = 54.5%	I = 46%
Interior (I) areas	B: E = 42%	B: E = 43%	B: E = 53%
	I = 58%	I =57%	I = 47%

frame a proximal portion of the exterior area which was considered "facing the nuclear boundary." The remaining portion of the exterior area of a territory was considered "not-facing" the nuclear boundary.

Statistical Analysis

To test the hypothesis of random placement, the exact 99% confidence intervals for p, the probability of a genetic locus signal located in the exterior area of a territory, was computed along with the point estimates. Confidence intervals which do not overlap 0.5 indicate rejection of the hypothesis with the significance level of 1%.

Results

The spatial position of three human genes coding for dystrophin (*DMD*), the β-myosin heavy chain (*MYH7*), and β-globin (*HBB*) in the nucleus was analyzed in cultured cells in which these genes are either active or inactive: in cultures of primary human myoblasts, myotubes generated by fusion of these myoblasts, primary human fibroblasts, and HeLa cells. Gene activity was assessed by amplification of mRNA applying reverse transcriptase PCR (RT-PCR) with primers from adjacent exons yielding positive PCR products only from spliced template RNA. The primers for the three genes as well as the constitutively expressed β-actin gene, *ACTB*, as a control, are presented in Table I. RT-PCR revealed expression of *DMD* and *MYH7* in myotubes as well as a low activity of *DMD* in the myoblast cultures, whereas *HBB* was not expressed in any of the cell cultures analyzed (see Fig. 1).

Analysis of the intranuclear position of genes requires three-dimensional preservation of the specimen. This was achieved by specialized protocols for the preparation of the analyzed cells that allow heat denaturation of chromosomes for FISH without disrupting the spatial organization of the genome in the nucleus. For establishing such a protocol, particular care was taken with respect to fixation and procedures facilitating probe penetration (protease digestion and alcohol reagents were avoided, since they are suspected to alter nuclear volumes). Preservation of the nuclear volume was judged by optical sectioning as well as scanning through the z-axis. In ellipsoid nuclei, the ratio of the z-axis extension to the x-y extension of the nucleus had to exceed 1/3 in order to accept a nucleus for the analysis. Assessment of the conservation of chromatin positioning was performed as shown in Fig. 2 (*A–C*). After a modest fixation (with 2% paraformaldehyde), kinetochores were stained using CREST autoantibodies and confocal images of stained nuclei were stored. After subsequent fixation with 4% paraformaldehyde and differential visualization of the centromeric sequences by FISH using alphoid probe DNA, images from the same optical sections
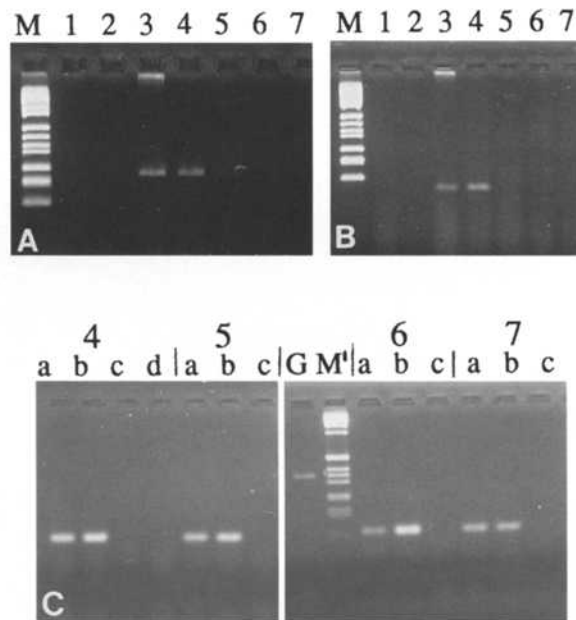
Figure 1. Analysis of gene expression by RT-PCR. The presence of mRNA of three genes, DMD (*A*), MYH7 (*B*), and HBB (*C*), was investigated in cultured primary human myoblasts, myotubes, fibroblasts, as well as in HeLa cells. Primers used for RT-PCR are indicated in Table I. *M*, size marker standard VI (Boehringer Mannheim); *M'*, 1 kb-ladder (BRL); *1*, myotube cDNA without PCR primer; *2*, reverse transcription with templates but PCR without template; *3*, total cDNA from human skeletal muscle; *4*, myotube cDNA; *5*, myoblast cDNA; *6*, fibroblast cDNA; *7*, HeLa cDNA; *G*, cosmid K40 (genomic DNA fragment containing HBBC) as template. For internal control, some experiments were performed with primer pairs specific for ACTB (*a*), ACTB and HBB (*b*), HBB alone (*c*), or without primer (*d*). DMD was found expressed in myotubes (*A*, lane *4*) and myoblasts (weak expression, not visible in *A*, lane *5*), and MYH7 was found only in myotubes (*B*, lane *4*). As shown in *C*, HBB was not expressed in any of the cell cultures, while the constitutively expressed β-actin gene, ACTB, served as a positive control in all cell types analyzed.

were acquired. Comparison of the staining before and after FISH, e.g., by electronic overlay of the images (see Fig. 2 *C*), confirmed the preservation of the nuclear architecture regarding the chromosome centromeres.

Delineation of chromosomal loci via FITC and chromosome territories via rhodamine was performed by applying dual color FISH. The probes used in this study are presented in Table I. After serial sectioning throughout each analyzed nucleus, the plane in which the spotlike FITC signal displayed maximal intensity was identified. Confocal images of FITC and rhodamine fluorescence were acquired in that particular focal plane and overlayed electronically. Examples of overlayed images are shown in Fig. 3. Separately acquired FITC and rhodamine images were overlayed to assess the localization of the gene signals within an interior or exterior part of the chromosome territory defined as described in Fig. 4 *A*: the signal is at the surface of the territory if the center of the signal is inside or outside of the territory border by not more than the diameter of the signal (exterior area); and the signal is within a territory, if it is inside of the region defined as the
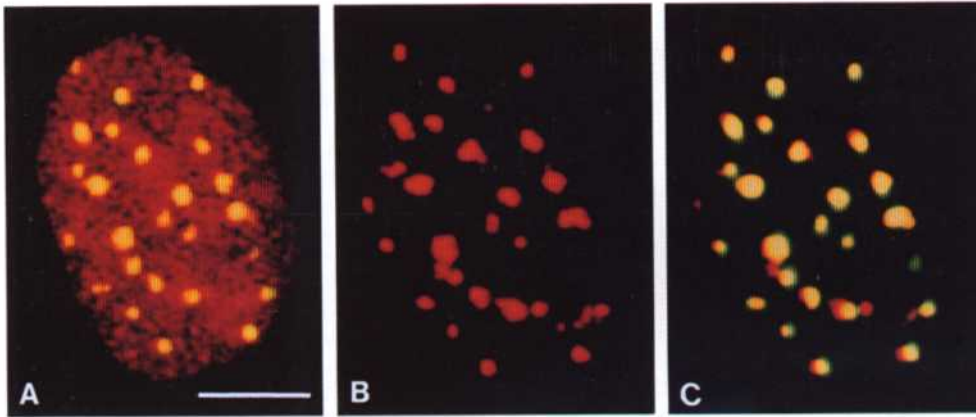
Figure 2. Assessment of the spatial conservation of nuclear chromatin arrangement during the FISH protocol. After modest paraformaldehyde fixation (see Materials and Methods section), kinetochores were stained with human CREST auto-antibodies, detected with FITC-conjugated anti-human antibodies, and images of optical sections were acquired using a confocal laser scanning microscope. After rigid fixation, permeabilization, and chromosomal denaturation, centromeres were visualized by FISH using a digoxigenin-labeled probe detecting the conserved 171-bp satellite DNA common to all human chromosome centromeres. After probe detection via rhodamine-conjugated anti-digoxigenin antibody, nuclei were relocated and images were taken from the same focal plane as before. (*A*) Confocal section of a HeLa nucleus with kinetochores visualized by indirect immunofluorescence (FITC) using CREST serum. The nucleus was counterstained with propidium iodide after the analysis shown in *B* and *C* was performed. (*B*) Image of the same focal plane of the nucleus shown in *A* with the centromeres stained by FISH. (*C*) Overlay of the CREST staining (*A*) and the FISH staining (*B*) of the centromeres reveal a colocalization of FITC and rhodamine fluorescence signals. Thus, the arrangement of chromosome centromeres in the nucleus remains conserved. Bar represents 5 μm.

surface (interior area). The diameter of the FITC signals of genetic loci analyzed in this study exhibited diameters of ~0.5–0.8 μm. Subsets of rhodamine images were interactively segmented without knowledge of the corresponding FITC image (see Fig. 4 *B*) by two independent investigators, in order to test the concordance regarding size, shape, and the resulting exterior/interior areas of chromosome territories. As shown in Table II, the concordance between the analysists was high, resulting in exterior and interior areas almost equal in size for medium-sized C-group chromosomes. Subsequent overlaying of the FITC and rhodamine images allowed the assignment of the locus derived signals to the exterior or interior areas of the territory as shown in Fig. 4 *C*. For illustration purposes, optical sections were also used to reconstruct a 3D image showing the spatial arrangement of genes with respect to the corresponding chromosome territories within a nucleus (kindly performed by C. Münkel, DKFZ, Heidelberg; see Fig. 4 *D*)

The spatial localization of three genes, *DMD*, *MYH7*, and *HBB*, with regard to their respective chromosome territories, was analyzed in four different cell types with different activity status of these genes (see above). For each combination of gene and cell type, 220–250 chromosome territories were evaluated. The gene-derived signal was always located within its territory, except for 0.6% (SD: 0.6%) of the signals found very close but not in direct contact to the signal of the territory (see Discussion). The subterritorial position of the analyzed genes is presented in Fig. 5. The vast majority of gene signals (73–88%) were located in the exterior area. The observed distribution of the gene signals was significantly different from the one expected if they were randomly located within the interior or exterior areas (see Table II). The statistical analysis revealed for all analyzed genes and cell types a rejection of the hypothesis of a random placement of the FITC signals at a significant value of 1%. Since for all three genes a similar preferential localization in the exterior area is found in all analyzed cell types, the localization is independent of the activity of the respective genes (see Fig. 5).

Since the ratio of the exterior area vs the interior area increases for the lower and upper optical sections through spherical chromosome territories, the results could be influenced by a localization of genes closer to the upper or lower planes of a given territory. However, the vertical intraterritorial position of the analyzed gene signals was carefully assessed for each cell type (see Table III) and only a small portion of the gene-derived signals was found within 1 μm of the upper and lower boundary of a territory. Furthermore, there was no significant difference of this distribution observed between the analyzed genes.

These data suggest a subterritorial organization, in which the genes are localized in the periphery of chromosome territories. To analyze the position of chromosomal segments not containing a gene, two other target regions were investigated in the same way: a clustered repetitive DNA sequence located on 1p36, D1Z2, which does not code for RNA, and an ~40-kb fragment from 11p14, designated 4-4B (see Table I). Northern blot analysis with total RNA from all analyzed cell types using cosmid 4-4B as a probe did not reveal any signal, even at very low stringency. Reprobing of the same filter with a β-actin control probe un-

Table III. Distribution of Gene Signals Along the Z-Axis of Chromosome Territories: Frequency of Signals Localized within the Upper and Lower X, Y-Sections*

	DMD	MYH7	HBB
		n = 200	
Myoblasts	8.5%	8%	8.5%
Myotubes	4%	10%	7%
Fibroblasts	8%	11.5%	16%
HeLa	6.5%	12%	8%

*Signals were scored when they were localized not more than 1 μm from the top or the bottom boundaries of the chromosome territories.
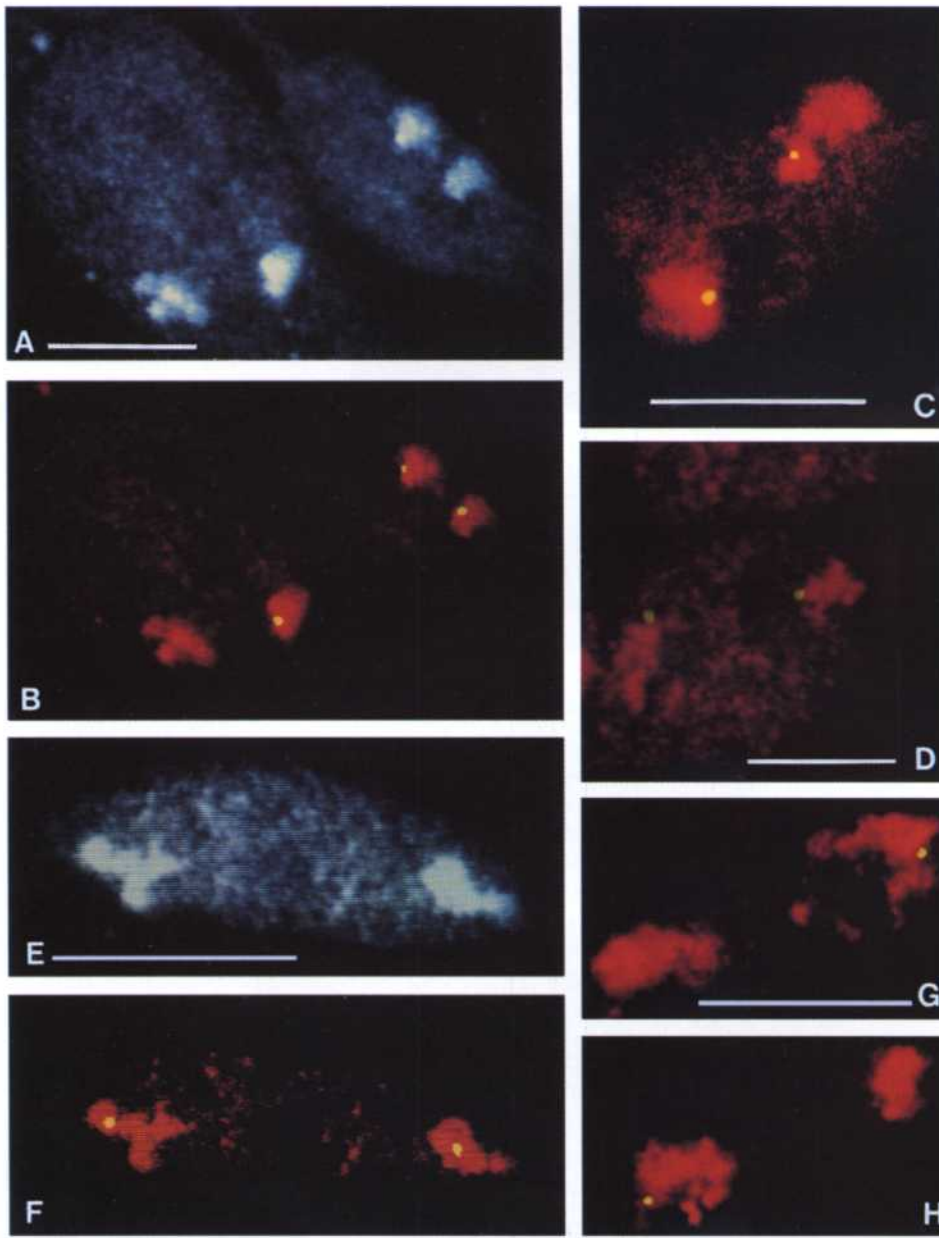
Figure 3. Visualization of genetic loci within their chromosome territories. The specific coding/noncoding sequences and their respective chromosome territories are differentially stained via FITC (*yellow/green*) and rhodamine (*red*), respectively, applying dual color FISH to three-dimensionally preserved nuclei. After serial sectioning throughout each analyzed nucleus, the plane in which the FITC signal displayed maximal intensity was identified. Confocal images of FITC and rhodamine fluorescence were acquired from that particular focal plane, overlaid and pseudocolored electronically. *A* and *E* present the original gray level images of the rhodamine fluorescence also contained in *B* and *F*, respectively, digitally enhanced to better illustrate the outline of the cell nuclei. (*A* and *B*) Visualization of the DMD gene within X chromosomes of primary human fibroblasts. (*A*) Section through four rhodamine-labeled X chromosome territories (two nuclei). (*B*) Same image as in *A* after overlaying of the FITC image acquired from the same focal plane and pseudocolorization. Note the localization of the three gene derived signals in the territorial periphery; the fourth gene signal is located in a different plane and therefore not visible. (*C*) Peripheral localization of DMD gene copies in X chromosomes of a HeLa cell nucleus. (*D*) Peripheral position of MYH7 within chromosome 14 territories in a nucleus of a human myotube. (*E* and *F*) Chromosome 11 territories in a myoblast nucleus (*E*) and the localization of the anonymous DNA fragment 4-4B from 11p14 (*F*). Note the localization of the FITC signals in the interior of the territories. (*G* and *H*) Visualization of the D1Z2 sequence, close to the telomere of 1p, and the chromosome 1 territories in a myoblast nucleus. The FITC signals are seen at the surface of the chromosomes. *G* and *H* represent different optical sections through the same nucleus, each with one D1Z2 signal in focus. Bars represent 10 µm.

der high stringency conditions resulted in the expected signals in all four cell types (data not shown).

Analysis of the position of D1Z2 within the territory of chromosome 1 revealed that, similar to the localization of the genes, D1Z2 was found in 68–77% of the cases in the exterior area (see Fig. 5). In contrast, between 39% and 49% of the signals from the cosmid probe 4-4B were found in the exterior area of chromosome 11 (see Fig. 5). Both probe signals were found in 2.3% of the cases (SD: 2.6%) close to but not overlapping with the chromosome territory signal. This distribution is clearly different from the other probes and resembles in myoblasts, myotubes, and fibroblasts a random distribution within the chromosome territory. This is confirmed by the statistical analysis which

could not reject the hypothesis of a random placement of the 4-4B signals in these three cell types at a significant value of 1%. However, in HeLa cells 4-4B is preferentially located in the interior area of the chromosome 11 territories as confirmed by the rejection of the hypothesis of a random placement of the 4-4B signals in the statistical analysis.

To analyze the positioning of the genes localized in the periphery of the chromosomes in more detail, the exterior area was further subdivided into two regions: one region was defined by the part of the chromosome territory boundary that is closest to the nuclear envelope, and the other region as the remaining part of the boundary (for a definition see the Materials and Methods section, for schematic illustration see Fig. 6 *A*). The distribution of the
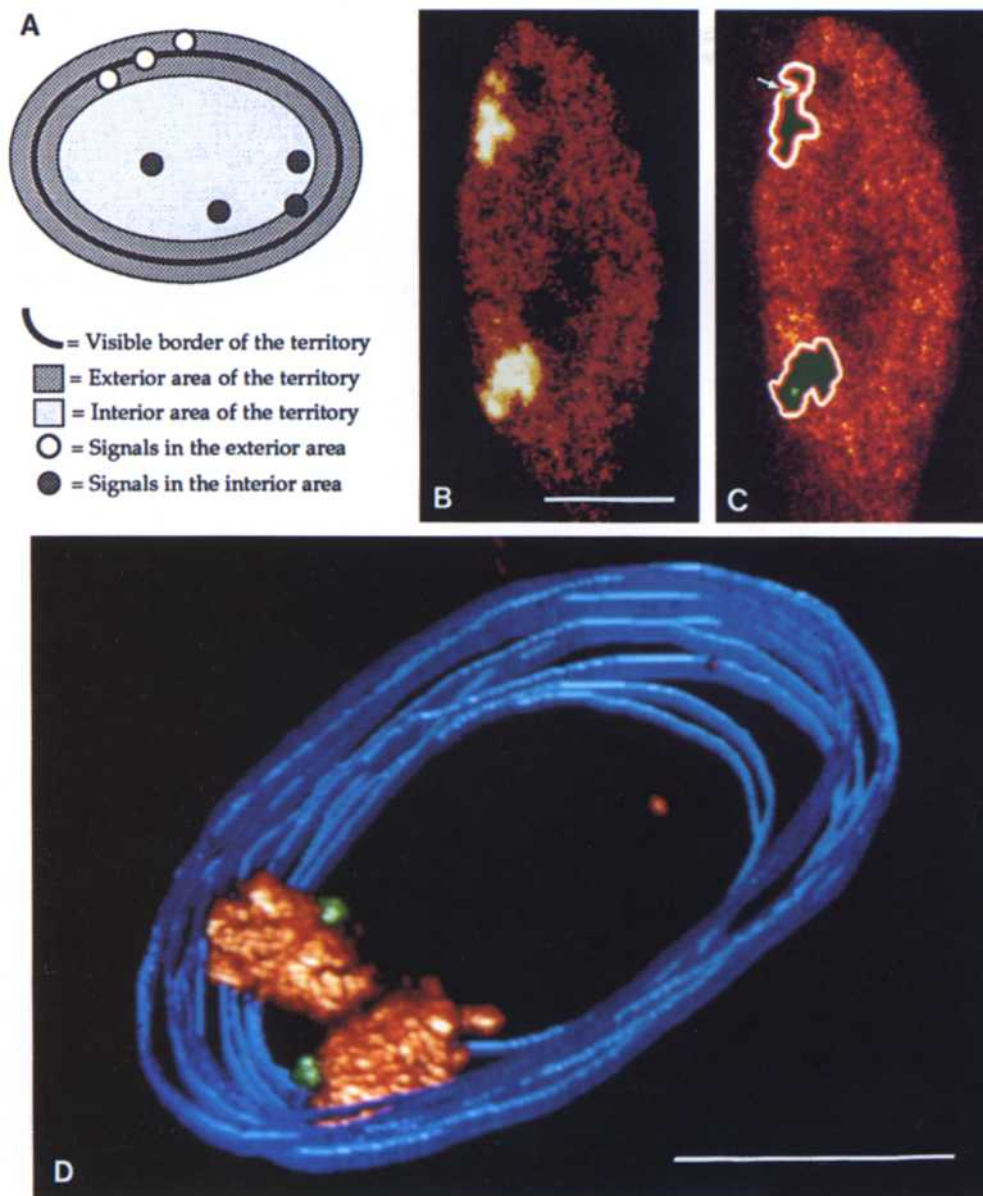
Figure 4. Three-dimensional analysis of genes within chromosome territories. (*A–C*) Segmentation of chromosome territories and definition of their exterior and interior areas. (*A*) Schematic illustration of a chromosome territory outlined by the bold line. The regions inside and outside of the territory border with a width equal to (or smaller than) the diameter of signals, which delineate gene-sized chromsomal segments, is considered an exterior area. The remaining region constitutes the interior area of a territory. (*B*) Example of a confocal section of a HeLa cell nucleus with two X chromosome territories delineated by FISH: such images were used to segment the chromosome territories interactively without knowing the position of the gene-derived signal (the latter was in the same focal plane, but its image was not overlaid and therefore not visible). (*C*) After interactive segmentation, the exterior and interior areas of each territory was calculated by using the measured diameter of the gene-derived signal (see *A*). The exterior area is composed of the region outside the segmentation line (*white*), as well as the region inside of the segmentation line with the same width (*red*). The interior area is shown in dark green. Subsequent overlay of the image containing the gene-derived signal (*bright green*) allowed the assignment of this signal to the exterior (upper territories in this example, see arrow) or interior (lower territories in this example) areas. (*D*) Illustration of the spatial arrangement of gene loci within chromosome territories after optical sectioning using a confocal laser scanning microscope. For this example, *DMD* gene copies were visualized simultaneously with the X chromosome territories in three-dimensionally preserved HeLa nuclei using dual color FISH. After parallel aquisition of FITC (*DMD*) and rhodamine (X chromosome) confocal images, pseudocolorization and electronic overlay, the nuclear border was outlined interactively and presented in blue for each optical section. Stacks of consecutive sections through labeled nuclei were used for the 3D reconstruction applying dedicated software. Bars represent 5 μm.

gene copies between these two subregions revealed highly characteristic patterns specific for *MYH7*, *DMD*, and *HBBC* (see Fig. 6, *B–D*). Statistical analysis of the dependence of this distribution of the gene copies from the analyzed genes and cell types using the generalized logit models (Agresti, 1990) showed that this distribution is only dependent from the genes. Since the most prominent feature is the localization of the *DMD* gene in the subregion proximal to the envelope, we determined the portion that this subregion presents within the exterior area analyzing a subset of 40 u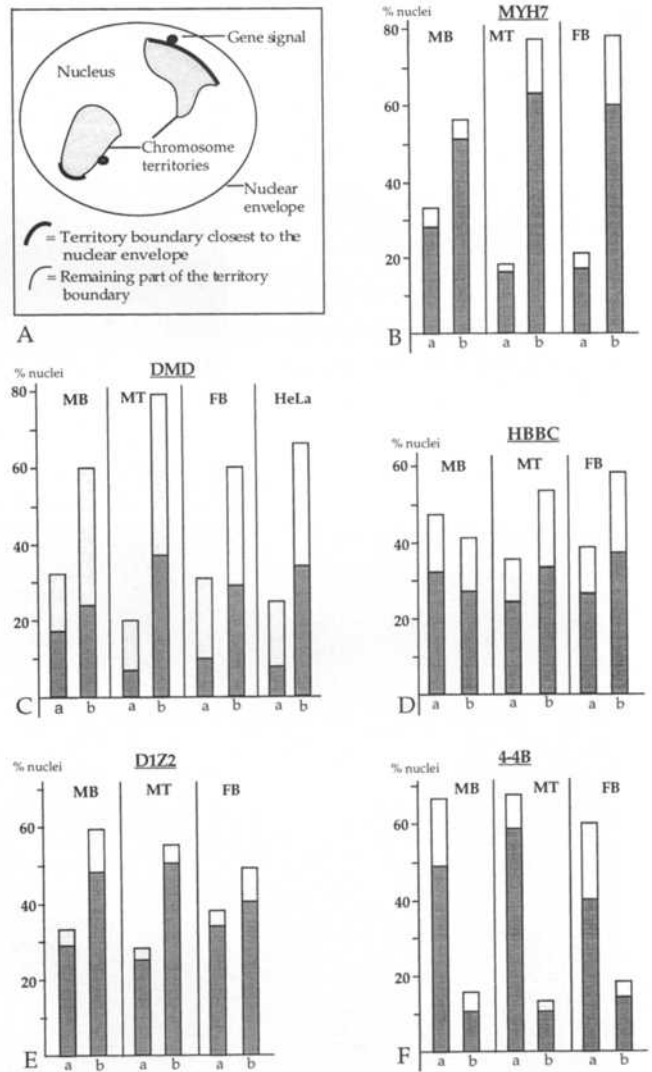nselected chromosome X territories. The proximal subregion was found to amount to an average of 30% of the exterior area. Since 55% of the *DMD* gene copies are found in this subregion (see Fig. 6 *C*), this again demonstrates that the localization is different from a random distribution. For the two noncoding DNA loci, different intraterritorial distributions were observed which were characteristic for each locus as well (Fig. 6, *E–F*). The spatial arrangement of the analyzed genes was again independent from their activity, since there was no significant difference in the number of gene copies found in proximity to the nuclear envelope, depending on the cell type.
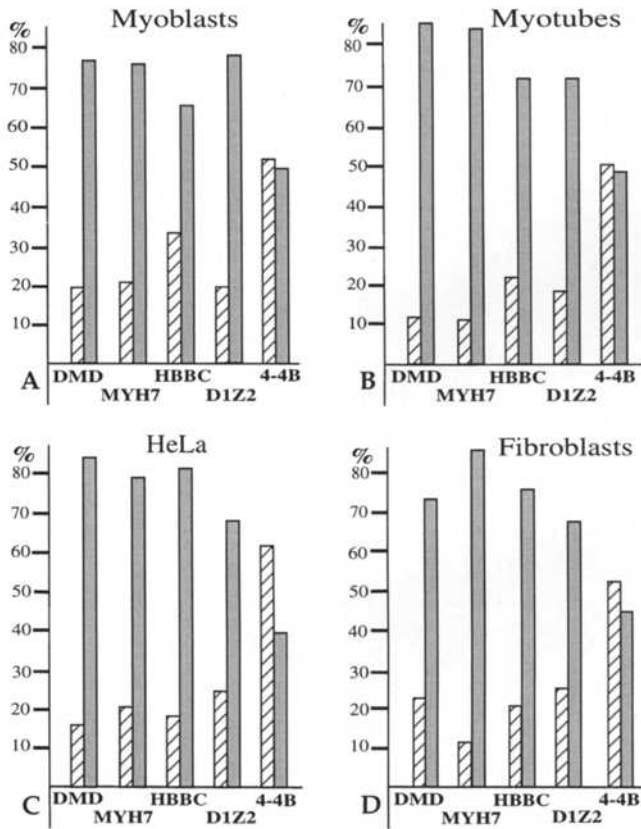
Figure 5. Distribution of the five analyzed genetic loci within the corresponding chromosome territories investigated in all four cell types (indicated). Hatched boxes represent the interior and gray boxes represent the exterior area (for each locus and cell type 220-250 chromosome territories were evaluated). Note the preferential localization of the gene- and D1Z2-derived signals in the exterior areas, whereas 4-4B–derived signals are equally distributed between both areas in three cell types (*A*, *B*, and *D*) and more frequently found in the interior area in HeLa cells (*C*). There is no striking difference in the positioning of the loci in the different cell types; the preferential distribution of the gene-derived signals (DMD, MYH7, and HBBC) in the exterior areas is not affected by the activation status of the corresponding genes. The distributions do not always add up to 100% since 0–6.3% of the signals could not be assigned to the exterior or interior region due to the location of the locus signal: (*a*) the signal was in a constriction of a waistlike shaped territory (i.e., the area of the constriction was smaller than FITC signal); or (*b*) the signal was close but not directly adjacent to the territory signal. For further explanation see text.

Discussion

Simultaneous visualization of chromosome territories and individual DNA segments in three-dimensionally preserved cell nuclei, applying dual color fluorescence in situ hybridization in combination with confocal laser scanning microscopy, provides a new avenue to study the spatial positioning of genes in the cell nucleus. Analysis of three genes revealed a preferential localization in the periphery of chromosome territories. In contrast, a noncoding segment of 11p14 was found predominantly localized in the interior area or randomly placed within the territory of chromosome 11. Many concepts of nuclear arrangement of

Figure 6. Subregional distribution of the analyzed loci located in the exterior area of the chromosome territories. (*A*) Schematic illustration of the two subregions of the exterior area defined by the proximity to the nuclear envelope as indicated and described in detail in the methods section. (*B–F*) Distribution of MYH7, DMD, HBBC, D1Z2, and 4-4B, respectively, between these two subregions in the different cell types, *MB*, myoblasts; *MT*, myotubes; *FB*, fibroblasts. The data are listed for nuclei with one (*a*) or both locus copies (*b*) in the exterior area of chromosome territories. Light gray boxes represent the localization of loci in the subregion, which is in proximity to the nuclear envelope; and dark boxes represent localization of loci in the other subregion. The percentages result from the analysis of 100 nuclei for each locus and cell type. Note that the distribution between the two subregions is highly characteristic for each locus. Since the HeLa line used in this study is heterogeneous with respect to the number of chromosomes 1, 11, and 14, only the DMD gene was analyzed in this cell line. The distributions do not add up to 100%. This is due to the reasons explained in the legend of Fig. 5, as well as to the fraction of nuclei where both alleles are located in the interior of the chromosome territories.

chromatin suggest a relationship between the activity of chromatin and certain topological features (Blobel, 1985; Hutchison and Weintraub, 1985; Jackson et al., 1993; Zirbel et al., 1993; van Driel and Verkleij, 1992; Cremer et al.,

1993; Spector et al., 1993; Xing et al., 1993; Pombo et al., 1994). In the present study no difference was found regarding the localization of genes whether they were active or inactive. Similarly, we identified localizations of genes within subregions of the exterior areas of chromosome territories that are not dependent on its activity. Thus, the subterritorial organization of the investigated genes, as detected on the level of light microscopy, was found to be characteristic for the genes but independent of their activity status.

It should be noted that the interpretation of data obtained by in situ hybridization and three-dimensional fluorescence microscopy has to take inherent methodological limitations into account. It is still not known to what extent chromatin arrangements observed after various fixation and in situ hybridization procedures reflect the in vivo situation. Preservation of the spatial organization of one group of chromosomal elements, the centromeres, was carefully monitored in our experiments, implying that the applied protocol is adequate for the investigation of the chromosome topology.

It also must be considered that the resolution of confocal microscopes is limited: while the lateral resolution is in the order of 0.3 μm or even better, the vertical resolution is in the range of 0.5–0.7 μm for the wavelengths of the emitting light from the fluorochromes used in the present study. However, optical sectioning with very small increments (0.1–0.2 μm) allowed a differentiation by the different signal intensities even of small gene-derived signals. Therefore, such sectioning was performed and only that particular section, which revealed maximum signal intensity, was used for the assessment of the subterritorial position of the signals.

Limitation of the optical resolution might greatly affect the ability to recognize special features of the spatial arrangement of small fluorescently labeled nuclear entities. Nevertheless, the localization of gene-derived signals was strongly deviating from a random positioning of genes within their chromosome territories. Thus, despite the inherent restrictions of the analysis procedure, the results of the present study provide strong evidence for a specific arrangement of the DNA string within interphase chromosomes.

The accurate determination of the boundaries of fluorescent signals, such as the painted chromosome territories, presents another problem crucial for the analysis performed in this study. The boundaries of fluorescently labeled chromosome territories are not always sharply edged. However, the high concordance of the interactive segmentation of chromosome territories between independent investigators (see Table II) showed that the reproducibility of the applied evaluation procedure was sufficient for the purpose of this study. More diffuse chromosome borders possibly reflect a lower density of chromatin, as for example by decondensed loops on the surface of chromosome territories. The small percentage of cases, where gene-derived or subtelomeric signals were close but not overlapping with the territory signal (0.6% and 2.3%, respectively) might reflect the rare occurrence of highly decondensed chromatin loops. A similar rare occurrence of gene derived signals which do not exactly overlap with a chromosome is also found on metaphase chromosomes fully delineated by chromosome banding, counterstaining,

or painting. These data indicate that entire interphase chromosomes could be faithfully delineated.

The confinement of genes to the peripheral area of chromosome territories implies a different arrangement of other sequences, such as certain noncoding sequences. Since the vast majority of genes is localized in Giemsa-light bands (R-bands), whereas Giemsa-dark bands (G-bands) are poor in gene content, an organization of the territories could be envisioned, where the G-bands are predominantly in the interior and the R-bands in the exterior area. After this rationale, sequences located in G-bands would not be expected to preferentially localize in the periphery of chromosome territories. Interestingly, the DNA fragment found to be located mostly in the interior or randomly distributed throughout the chromosome territory is localized within one of the largest G-bands of human chromosomes (11p14). The localization of the locus D1Z2 mostly at the periphery of the chromosome territory is also compatible with this model: although a noncoding sequence, it is localized in the telomeric band of human chromosome 1p, which is an R-band. Notably, almost all human telomeric bands constitute R-bands and telomeres are shown to be often associated with the nuclear envelope (Manuelidis and Borden, 1988; Mathog et al., 1984; Katsumata and Lo, 1988; Rawlins and Shaw, 1990; Rawlins et al., 1991; Zalensky et al., 1995).

Measurement of nuclear distances between physically linked DNA sequences, separated by 0.1–2 Mbp, which were visualized by FISH (Lawrence et al., 1988; Trask et al., 1989), provided the basis for the so-called "random walk model" (van den Engh et al., 1992). Further measurements of interphase distances between chromosomal points up to 190 Mbp apart from each other lead to the extension to the so-called random walk/giant loop model. According to this model, DNA is randomly folded within loops several Mbp in size, and the loops are organized along a backbone again in a random manner (Yokota et al., 1995; Sachs et al., 1995). Here, the reported preferential positioning of genes and their characteristic orientation with regard to the nuclear envelope seem difficult to fit to the predictions of the random walk/giant loop model. When comparing our data with this model, the following issues need to be considered: (a) the intranuclear distances, providing the basis for this model, were only measured in a two-dimensional way by using either very flat nuclei for the analysis (often not well spatially preserved, since they were mostly fixed in methanol/acetic acid, swollen in hypotonic solutions and spread out on glass surfaces), or by projecting loci in spatially preserved specimen onto a two-dimensional area; (b) in the interphase studies from which the random walk/giant loop model were concluded, the positioning of the visualized DNA segments was not analyzed with respect to chromosome territories; (c) distance measurements between two points, one of which is specifically positioned (e.g., a gene in a territory) whereas the other one is not (e.g., another segment in a territory), likely results in highly variable values supportive for a random walk model; (d) the present study reveals a characteristic intraterritorial localization of genes; however, this localization is not fixed to distinct spatial coordinates, but refers to a large region within the territory (~50%), and it could well be that the preferential localization in such a large area

does not become apparent from the two-dimensional distance measurements of multiple pairs of loci; (e) the linear relationship of the physical distance and the interphase distance between certain points of the territorially arranged DNA string might as well be explained by alternative nonrandom walk models.

The original concept of confinement of transcription to the nuclear periphery (Hutchison and Weintraub, 1985) could not be confirmed by other investigators analyzing the nuclear distribution of DNAase hypersensitive sites (Manuelidis and Borden, 1988) or newly synthesized RNA-polymerase II transcripts detected by pulsed BrUTP incorporation (Jackson et al., 1993; Wansink et al., 1993; Pombo et al., 1994). The latter were found in clusters scattered throughout the nucleus. Despite the description of defined nuclear subregions for transcription sites, little is known regarding the structural basis of the formation of these subregions. One clue might be provided by the findings of the present study. The observed placement of genes should result in the localization of newly synthesized RNA in the periphery of chromosome territories, and indeed such an arrangement of RNA was found in an analysis of the spatial relationship of HPV18 RNA with the chromosome 8 territory in HeLa cells, which contains the integrated HPV-DNA (Zirbel et al., 1993). Since it was shown that genes can be spatially associated with their RNA products in the nucleus (Xing et al., 1993), these findings are in concordance with the localization of coding sequences in the periphery of the chromosome territories.

The localization of genes in the exterior area of the chromosome territories concurs in a previously proposed model of a nuclear compartment for gene transcription, RNA processing, and RNA transport defined by the periphery of chromosome territories, the inter-chromosome-domain (ICD) compartment (Zirbel et al., 1993; Cremer et al., 1993). According to this model, the surface areas of adjacent chromosome territories define a structural and functional compartment, where genes are exposed. After transcription, RNA polymerase II products would be released into the compartment, where they are processed and transported to the nuclear pores also connected to the ICD space.

Consideration of the spatial relation of coding sequences and chromosome territories provides a novel approach that could serve as a paradigm for 3D genome analyses. Further analyses, including an increased number of coding and noncoding sequences, are required to test the various models for the intraterritorial arrangement of the DNA string, and to better understand the three-dimensional organization of complex genomes.

References

Agresti, A. 1990. Categorical Data Analysis. John Wiley & Sons, New York.

Akoury, D.A., J.J. Seo, C.D. James, and S.R. Zaki. 1993. RT-PCR detection of mRNA recovered from archival glass slide smears. Mod. Pathol. 6:195–200.

Arndt-Jovin, D.J., M. Robert-Nicaud, and T.M. Jovin. 1990. Probing DNA structure and function with a multiwavelength fluorescence confocal laser microscope. J. Microsc. 157:131–139.

Barr, M., and E.G. Bertram. 1951. Behavior of nuclear structures during depletion and restoration of Nissl material in motor neurons. J. Anat. (Lond.). 85:171–181.

Belmont, A.S., M.B. Braunfeld, J.W. Sedat, and D.A. Agard. 1989. Large-scale chromatin structural domains within mitotic and interphase chromosomes in vivo and in vitro. Chromosoma. 98:129–143.

Berman, S.A., S. Bursztajn, B. Bowen, and W. Gilbert. 1990. Localization of an acetylcholine receptor intron to the nuclear membrane. Science (Wash. DC). 247:212–214.

Bertram, E.G. 1966. Behavior of the sex chromatin during altered states of cell metabolism. In The Sex Chromatin. K.L. Moore, editors. W.B. Saunders Company, Philadelphia, London. 162–172.

Blobel, G. 1985. Gene gating: a hypothesis. Proc. Natl. Acad. Sci. USA. 82:8527–8529.

Borden, J., and L. Manuelidis. 1988. Movement of the X chromosome in epilepsy. Science (Wash. DC). 242:1687–1691.

Brasch, K. 1990. Drug and metabolite-induced perturbations in nuclear structure and function: a review. Biochem. Cell Biol. 68:408–426.

Buroker, N., R. Bestwick, G. Haight, R.E. Magenis, and M. Litt. 1987. A hypervariable repeated sequence on human chromosome 1p36. Hum. Genet. 77:175–181.

Carmo-Fonseca, M., D. Tollervey, R. Pepperkok, S.M.L. Barabino, A. Merdes, C. Brunner, P.D. Zamore, M.R. Green, E. Hurt, and A.I. Lamond. 1991. Mammalian nuclei contain foci which are highly enriched in components of the pre-mRNA splicing machinery. EMBO (Eur. Mol. Biol. Organ.) J. 10:195–206.

Carter, K.C., K.L. Taneja, and J.B. Lawrence. 1991. Discrete nuclear domains of poly(A)RNA and their relationship to the functional organization of the nucleus. J. Cell Biol. 115:1191–1202.

Collins, C., W.L. Kuo, R. Segraves, J. Fuscoe, D. Pinkel, and J. Gray. 1991. Construction and characterization of plasmid libraries enriched in sequences from single human chromosomes. Genomics. 11:997–1006.

Collins, F.S., and S.M. Weissman. 1984. The molecular genetics of human hemoglobin. Prog. Nucleic Acid Res. Mol. Biol. 31:315–465.

Comings, D.E. 1968. The rationale for an ordered arrangement of chromatin in the interphase nucleus. Am. J. Hum. Genet. 20:440–460.

Comings, D.E. 1980. Arrangement of chromatin in the nucleus. Hum. Genet. 53:131–143.

Cremer, T. 1985. Von der Zellenlehre zur Chromosomentheorie. Springer Verlag, Heidelberg. 384 pp.

Cremer, T., C. Cremer, T. Schneider, H. Baumann, L. Hens, and M. Kirsch-Volders. 1982. Analysis of chromosome positions in the interphase nucleus of Chinese hamster cells by laser-UV-microirridiation experiments. Hum. Genet. 62:201–209.

Cremer, T., A. Kurz, R. Zirbel, S. Dietzel, B. Rinke, E. Schröck, M.R. Speicher, U. Mathieu, A. Jauch, P. Emmerich, et al. 1993. The role of chromosome territories in the functional compartmentalization of the cell nucleus. Cold Spring Harbor Symp. Quant. Biol. 58:777–792.

Cremer, T., P. Lichter, J. Borden, D.C. Ward, and L. Manuelidis. 1988. Detection of chromosome aberrations in metaphase and interphase tumor cells by in situ hybridization using chromosome specific library probes. Hum. Genet. 80:235–246.

Dunham, I., C. Lengauer, T. Cremer, and T. Featherstone. 1992. Rapid generation of chromosome specific alphoid DNA probes using the polymerase chain reaction. Human Genet. 88:457–462.

Ehrenpreis, J., M. Hillers, B. Junkes, M. Pfordt, E. Schwinger, and H.-P. Vosberg. 1991. Analysis of a dystrophin gene deletion by amplification of mRNA isolated from DMD myotubes cultured in vitro. Genomics. 10:551–557.

Ferguson, M., and D.C. Ward. 1992. Cell cycle dependent chromosomal movement in pre-mitotic human T-lymphocyte nuclei. Chromosoma. 101:557–565.

Gasser, S.M., and U.K. Laemmli. 1987. A glimpse at chromosomal order. TIG. 3:16–22.

Graham, G.A. 1954. Sex chromatin in cell nuclei of the cat from the early embryo to maturity. Anatomical Record. 119:469–491.

Gunning, P., P. Ponte, H. Okoyama, J. Engel, H. Blau, and L. Kedes. 1983. Isolation and characterization of full-length cDNA clones for human α-, β- and γ-actin mRNAs: skeletal but not cytoplasmic actins have an amino terminal cysteine that is subsequently removed. Mol. Cell. Biol. 3:787–795.

Haaf, T., and M. Schmid. 1991. Chromosome topology in mammalian interphase nuclei. Exp. Cell Res. 192:325–332.

Heslop-Harrison, J.S., and M.D. Bennett. 1984. Chromosome order — possible implications for development. J. Embryol. Exp. Morph. 83: (Suppl.) 51–73.

Hilliker, A.J., and R. Appels. 1989. The arrangement of interphase chromosomes: structural and functional aspects. Exp. Cell Res. 185:297–318.

Hochstrasser, M., and J.W. Sedat. 1987. Three-dimensional organization of Drosophila melanogaster interphase nuclei. II. Chromosome spatial organization and gene expression. J. Cell Biol. 104:1471–1482.

Huang, S., and D.L. Spector. 1991. Nascent pre-mRNA transcripts are associated with nuclear regions enriched in splicing factors. *Genes Dev.* 5:2288–2302.

Hutchison, N., and H. Weintraub. 1985. Localization of DNAse I-sensitive sequences to specific regions of interphase nuclei. *Cell.* 43:471–482.

Jackson, D.A., A.B. Hassan, R.J. Errington, and P.R. Cook. 1993. Visualization of focal sites of transcription within human nuclei. *EMBO (Eur. Mol. Biol. Organ.) J.* 12:1059–1065.

Jiménez-Garcia, L.F., and D.L. Spector. 1993. In vivo evidence that transcription and splicing are coordinated by a recruiting mechanism. *Cell.* 73:47–59.

Junkes-Biehl, B. 1992. Expression von Myosin-Isoformen in humanen Muskelzellen in vitro. *Thesis Univ. Heidelberg.*

Katsumata, M., and C.W. Lo. 1988. Organisation of chromosomes in the mouse nucleus: analysis by in situ hybridization. *J. Cell Sci.* 90:193–199.

Lawrence, J.B., R.H. Singer, and L.M. Marselle. 1989. Highly localized tracks of specific transcripts within interphase nuclei visualized by in situ hybridization. *Cell.* 57:493–502.

Lawrence, J.B., C.A. Villnave, and R.H. Singer. 1988. Interphase chromatin and chromosome gene mapping by fluorescence detection of in situ hybridization reveals the presence and orientation of two closely integrated copies of EBV in a human lymphoblastoid cell line. *Cell.* 52:51–61.

Leitch, A.R., W. Mosgöller, T. Schwarzacher, M.D. Bennett, and J.S. Heslop-Harrison. 1990. Genomic in situ hybridization to sectioned nuclei shows chromosome domains in grass hybrids. *J. Cell Sci.* 95:335–341.

Lichter, P., T. Cremer, J. Borden, L. Manuelidis, and D.C. Ward. 1988*a*. Delineation of individual human chromosomes in metaphase and interphase cells by in situ suppression hybridization using recombinant DNA libraries. *Hum. Genet.* 80:224–234.

Lichter, P., T. Cremer, C.C. Tang, P.C. Watkins, L. Manuelidis, and D.C. Ward. 1988*b*. Rapid detection of human chromosome 21 aberrations by in situ hybridization. *Proc. Natl. Acad. Sci. USA.* 85:9664–9668.

Lichter, P., S.A. Ledbetter, D.H. Ledbetter, and D.C. Ward. 1990*a*. Fluorescence in situ hybridization with Alu and L1 polymerase chain reaction probes for rapid characterization of human chromosomes in hybrid cell lines. *Proc. Natl. Acad. Sci. USA.* 87:6634–6638.

Lichter, P., C.C. Tang, K. Call, G. Hermanson, G.A. Evans, D. Housman, and D.C. Ward. 1990*b*. High resolution mapping of human chromosome 11 by in situ hybridization with cosmid clones. *Science (Wash. DC).* 247:64–69.

Lichter, P., P.K. Umeda, J.E. Levin, and H.-P. Vosberg. 1986. Partial characterization of the human β-myosin heavy chain gene which is expressed in heart and skeletal muscle. *Eur. J. Biochem.* 160:419–426.

Lindenbaum, R.H., G. Clarke, C. Patel, M. Moncrieff, and J.T. Hughes. 1979. Muscular dystrophy in an X;1 translocation female suggests that Duchenne locus is on X chromosome short arm. *J. Med. Genet.* 16:389–392.

Manuelidis, L. 1984. Different central nervous system cell types display distinct and nonrandom arrangements of satellite DNA sequences. *Proc. Natl. Acad. Sci. USA.* 81:3123–3127.

Manuelidis, L. 1985. Individual interphase chromosome domains revealed by in situ hybridization. *Hum. Genet.* 71:288–293.

Manuelidis, L. 1990. A view of interphase chromosomes. *Science (Wash. DC).* 250:1533–1540.

Manuelidis, L., and J. Borden. 1988. Reproducible compartmentalization of individual chromosome domains in human CNS cells revealed by in situ hybridization and three-dimensional reconstruction. *Chromosoma.* 96:397–410.

Mathog, D., M. Hochstrasser, and J.W. Sedat. 1984. Characteristic folding pattern of the polytene chromosomes in Drosophila salivary gland nuclei. *Nature (Lond.).* 308:414–421.

Matsuoka, R., M.C. Yoshida, N. Kanda, M. Kimura, H. Ozasa, and A. Takao. 1989. Human cardiac myosin heavy chain gene mapped within chromosome region 14q11.2-q13. *Am. J. Med. Genet.* 32:279–284.

Morton, C.C., I.R. Kirsch, R. Taub, S.H. Orkin, and J.A. Brown. 1984. Localization of the β-globin gene by chromosomal in situ hybridization. *Am. J. Hum. Genet.* 36:576–585.

Nyman, U., H. Hallman, G. Hadlaczky, I. Pettersson, G. Sharp, and N.R. Ringertz. 1986. Intranuclear localization of snRNP antigens. *J. Cell Biol.* 102:137–144.

Pinkel, D., J. Landegent, C. Collins, J. Fuscoe, R. Segraves, J. Lucas, and J.W. Gray. 1988. Fluorescence in situ hybridization with human chromosome-specific libraries: detection of trisomy 21 and translocations of chromosome 4. *Proc. Natl. Acad. Sci. USA.* 85:9138–9142.

Pombo, A., J. Ferreira, E. Bridge, and M. Carmo-Fonseca. 1994. Adenovirus replication and transcription sites are spatially separated in the nucleus of infected cells. *EMBO (Eur. Mol. Biol. Organ.) J.* 13:5075–5085.

Raap, A.K., F.M. van de Rijke, R.W. Dirks, C.J. Sol, R. Boom, and M. van der Ploeg. 1991. Bicolor fluorescence in situ hybridization to intron and exon mRNA sequences. *Exp. Cell Res.* 197:319–322.

Rawlins, D.J., M.I. Highett, and P.J. Shaw. 1991. Localization of telomeres in plant interphase nuclei by in situ hybridization and 3D confocal microscopy. *Chromosoma.* 100:424–431.

Rawlins, D.J., and P.J. Shaw. 1990. Localization of ribosomal and telomeric DNA sequences in intact plant nuclei by in situ hybridization and three dimensional optical microscopy. *J. Microsc.* 157:83–89.

Sachs, R.K., G. van den Engh, B. Trask, H. Yokota, and J.E. Hearst. 1995. A random-walk giant-loop model for interphase chromosomes. *Proc. Natl. Acad. Sci. USA.* 92:2710–2714.

Saiki, R.K., S. Scharf, F. Faloona, K.B. Mullis, G.T. Horn, A.H. Erlich, and N. Arnheim. 1985. Enzymatic amplification of β-globin genomic sequences and restriction site analysis for diagnosis of sickle cell anemia. *Science (Wash. DC).* 230:1350–1354.

Sambrook, J., E.F. Fritsch, and T. Maniatis 1989. Molecular Cloning. A Laboratory Manual. Cold Spring Harbor Laboratory Press, Cold Spring Harbor, New York. pp. 7.3–7.86.

Schardin, M., T. Cremer, H.D. Hager, and M. Lang. 1985. Specific staining of human chromosomes in Chinese hamster x man hybrid cell lines demonstrates interphase chromosome territories. *Hum. Genet.* 71:281–287.

Schmid, M., and W. Krone. 1976. The relationship of a specific chromosomal region to the development of the acrosome. *Chromosoma.* 56:327–347.

Schwarzacher, T., A.R. Leitch, M.D. Bennett, and J.S. Heslop-Harrison. 1989. In situ localization of parental genomes in a wide hybrid. *Ann. Bot.* 64:315–324.

Spector, D.L. 1990. Higher order nuclear organization: three-dimensional distribution of small nuclear ribonucleoprotein particles. *Proc. Natl. Acad. Sci. USA.* 87:147–151.

Spector, D.L., S. Landon, and R.T. O'Keefe. 1993. Organization of RNA polymerase II transcription and pre-mRNA splicing within the mammalian cell nucleus. *Cold Spring Harbor Symp. Quant. Biol.* 21:918–920.

Spiegelberg, R., C. Aulehla-Scholz, H. Erlich, and J. Horst. 1989. A β-thalassemia gene caused by a 290 bp deletion: analysis by direct sequencing of enzymatically amplified DNA. *Blood.* 73:1695–1698.

Tocharoentanaphol, C., M. Cremer, E. Schröck, L. Blonden, K. Kilian, T. Cremer, and T. Ried. 1994. Multicolor fluorescence in situ hybridization on metaphase chromosomes and interphase halo preparations using cosmid and YAC clones for the simultaneous high resolution mapping of deletions in the dystrophin gene. *Hum. Genet.* 93:229–235.

Trask, B., D. Pinkel, and G. van den Engh. 1989. The proximity of DNA sequences in interphase cell nuclei is correlated to genomic distance and permits ordering of cosmids spanning 250 kilobase pairs. *Genomics.* 5:710–717.

van den Engh, G., R. Sachs, and B. Trask. 1992. Estimating genomic distances from DNA sequence location in cell nuclei by a random walk model. *Science (Wash. DC).* 257:1410–1412.

van Driel, R., and A. Verkleij. 1992. The cell nucleus, the unexplored organelle. *Cell Biol. Int. Rep.* 16:683–685.

Vogel, F., and T.M. Schroeder. 1974. The internal order of the interphase nucleus. *Humangenetik.* 25:265–297.

Wansink, D.G., W. Schul, I. van der Kraan, B. van Steensel, R. van Driel, and L. de Jong. 1993. Fluorescent labeling of nascent RNA reveals transcription by RNA polymerase II in domains scattered throughout the nucleus. *J. Cell Biol.* 122:283–293.

Xing, Y., C.V. Johnson, P.R. Dobner, and J.B. Lawrence. 1993. Higher level organization of individual gene transcription and RNA splicing. *Science (Wash. DC).* 259:1326–1330.

Yokota, H., G. van den Engh, J.E. Hearst, R.K. Sachs, and B.J. Trask. 1995. Evidence for the organization of chromatin in megabase pair-sized loops arranged along a random-walk path in the human G0/G1 interphase nucleus. *J. Cell Biol.* 130:1239–1249.

Zalensky, A.O., M.J. Allen, I.A. Kobayashi, I.A. Zalenskaya, R. Balhorn, and E.M. Bradbury. 1995. Well-defined genome architecture in the human sperm nucleus. *Chromosoma.* 103:577–590.

Zirbel, R.M., U.R. Mathieu, A. Kurz, T. Cremer, and P. Lichter. 1993. Evidence for a nuclear compartment of transcription and splicing located at chromosome domain boundaries. *Chrom. Res.* 1:93–106.

Zorn, C., C. Cremer, T. Cremer, and J. Zimmer. 1979. Unscheduled DNA synthesis after partial UV irradiation of the cell nucleus. *Exp. Cell Res.* 124:111–119.